The Human Erythrocyte Sugar Transporter Presents Two Sugar Import Sites†

Stephanie Hamill, Erin K. Cloherty, and Anthony Carruthers*

Department of Biochemistry and Molecular Biology, University of Massachusetts Medical School, 55 Lake Avenue North, Worcester, Massachusetts 01655

Received August 11, 1999

ABSTRACT: The human erythrocyte sugar transporter presents sugar import (e2) and sugar export (e1) sites simultaneously. This study asks whether the sugar transporter exposes only one or multiple import sites. We approached this question by analysis of cytochalasin B binding to the human erythrocyte sugar export site in the presence of sugars that bind to the sugar import site. Extracellular maltose does not enter human erythrocytes. High concentrations of maltose (1−100 mM) inhibit cytochalasin B binding to human red cells. Low concentrations (25−500 μM) increase the level of erythrocyte cytochalasin B binding. Maltose modulation of cytochalasin B binding is mediated by altered affinity of sugar export sites for cytochalasin B. Similar results are obtained with other cell-impermeant inhibitors of sugar uptake. Extracellular D-glucose (a transported sugar) stimulates cytochalasin B binding at low D-glucose concentrations (10−250 μM), but this effect is lost at higher concentrations. Intracellular D-glucose inhibits cytochalasin B binding. Low concentrations of extracellular maltose and other nontransported inhibitors stimulate 3-*O*-methylglucose uptake in erythrocytes. Higher sugar concentrations (1−100 mM) inhibit transport. These data support the hypothesis that the erythrocyte sugar transporter presents two sugar import sites and at least one sugar export site. This conclusion is consistent with the proposed oligomeric structure of the sugar transporter, a complex of four GluT1 proteins in which each subunit presents a translocation pathway.

The human erythrocyte sugar transporter is comprised of four copies of the glucose transport protein GluT1[1] (*1*, *2*). This complex functions as a fixed-site carrier (*3*, *4*) presenting sugar import and sugar export sites simultaneously (*5*). It has been proposed (*6*) that each sugar transport site is contributed by a single GluT1 subunit which alternates between import (e2) and export (e1) competent states (*6*, *7*). Depending upon the nature of the occupying ligands, sugar import and sugar export sites exhibit varying degrees of positive or negative cooperativity (*5*).

Several observations suggest that a cooperative fixed-site carrier mechanism cannot fully account for the sugar transport properties of human erythrocytes. Unidirectional sugar efflux from red cells into medium containing saturating sugar levels is characterized by a $K_{m(app)}$ that is almost 1 order of magnitude lower than that predicted by the cooperative fixed-site carrier mechanism (*8*). $K_{m(app)}$ for unidirectional 3-*O*-methylglucose (3OMG) uptake by red cells containing saturating 3OMG levels is significantly greater than $K_{i(app)}$ for extracellular 3OMG inhibition of net 3OMG exit (*9*). Naftalin (*10*) has demonstrated that sugar binding to the human erythrocyte glucose transporter can lead to an activated state which remains transiently activated after glucose dissociation. These observations suggest that the human erythrocyte sugar transporter presents additional sugar binding sites or that the exofacial sugar binding site cycles between high- and low-affinity states.

This study examines the hypothesis that the human erythrocyte sugar transporter contains only one exofacial sugar binding site. We monitored extracellular sugar binding to the glucose transporter in red cells by analysis of the effects of extracellular sugars on cytochalasin B binding to the sugar export site and by examination of extracellular sugar modulation of 3-*O*-methylglucose uptake. Our findings support rejection of the single-exofacial sugar binding site hypothesis and are consistent with a mechanism in which sugar binding to a high-affinity, exofacial site promotes cytochalasin B binding at the sugar export site and sugar translocation through a second import site.

MATERIALS AND METHODS

Materials. Human blood was obtained from the American Red Cross. Radiochemicals were purchased from New England Nuclear (Boston, MA). All other reagents were purchased from Sigma Chemical Co. (St. Louis, MO).

Solutions. Saline consisted of 150 mM NaCl, 10 mM Tris-HCl, and 0.5 mM EDTA (pH 7.4). Lysis medium contained 10 mM Tris-HCl and 0.2 mM EDTA (pH 7.2). Stop solution consisted of ice-cold saline with 10 μM CCB and 100 μM phloretin.

Red Cells. Red cells were isolated from whole human blood by repeated wash−centrifugation cycles in ice-cold

† This work was supported by NIH Grant DK 44888.

* To whom correspondence should be addressed. E-mail: anthony.carruthers@umassmed.edu. Telephone: (508) 856-5570. Fax: (508) 856-6231.

[1] Abbreviations: GluT1, human erythrocyte glucose transport protein; 3OMG, 3-*O*-methylglucose; CCB, cytochalasin B; CCD, cytochalasin D; EDTA, ethylenediaminetetraacetic acid; EGTA, ethylene glycol bis-(β-aminoethyl ether)-*N*,*N*,*N*′,*N*′-tetraacetic acid; Tris-HCl, tris(hydroxymethyl)aminomethane.

10.1021/bi9918792 CCC: $18.00
Published on Web 12/02/1999

saline. One volume of whole blood was mixed with 3 volumes of saline and the mixture centrifuged at 10000*g* for 5 min at 4 °C. Serum and the buffy coat were aspirated, and the wash−centrifugation cycle was repeated until the supernatant was clear and the buffy coat was no longer visible.

Erythrocyte Membrane Ghosts. Washed red cells were lysed in 40 volumes of lysis medium, incubated on ice for 10 min, and then centrifuged at 22000*g* for 20 min at 4 °C. The supernatant was aspirated, and the lysis−centrifugation−aspiration cycle was repeated. The resulting membranes were resealed by incubation in KCl medium containing or lacking 4 mM MgATP (pH 7.4) at 37 °C for 60 min and harvested by centrifugation at 22000*g* for 20 min at 4 °C.

Cytochalasin B Binding. Red cells were depleted of endogenous sugars by incubation at 37 °C in 40 volumes of sugar-free saline. Cells were then preincubated with various sugars at varying concentrations for 20 min at 37 °C. Cells were harvested by centrifugation (14000*g* for 5 min at 4 °C) and resuspended in saline (22 °C) containing (1) sugar species at concentrations identical to those in the preincubation condition or (2) [^{3}H]CCB (6 μCi/mL), 100 nM unlabeled CCB, and 10 μM CCD. This suspension was incubated for 20 min at 22 °C, and the extent of [^{3}H]-cytochalasin B binding was determined by a centrifugation procedure (*8*).

Briefly, pelleted, preincubated cells were resuspended by addition of 120 μL of medium containing [^{3}H]cytochalasin B. Aliquots (20 μL) of the suspension were counted by liquid scintillation spectroscopy using a Beckman scintillation counter. This provides a measure of the "total" suspension cytochalasin B concentration. Cells were incubated for 30 min at 22 °C with end-over-end rotation, by which time equilibrium cytochalasin B binding is achieved (*11*). The cell suspension was centrifuged at 14000*g* for 20 s, and aliquots (20 μL) of the clear supernatant were assessed by liquid scintillation spectroscopy. This provides a measure of the "free" cytochalasin B concentration. The bound cytochalasin B concentration is computed as total − free cytochalasin B concentration. All counts were corrected for quenching-induced errors and are expressed as disintegrations per minute.

Net 3-O-Methylglucose Uptake. Sugar transport by red cells was as described previously (*12*). Briefly, sugar-free cells or resealed erythrocyte ghosts at ice temperature were exposed to 5 volumes of ice-cold KCl medium containing [^{3}H]-3-*O*-methylglucose and variable concentrations of unlabeled 3-*O*-methylglucose and/or competing sugar. The rate of uptake was measured over intervals of 15 s to 1 min, and then 50 volumes (relative to cell volume) of ice-cold stopper solution was added to the cell/ghost suspension. The cells and ghosts were sedimented by centrifugation (14000*g* for 30 s), washed once in stopper, collected by centrifugation, and extracted in 500 μL of 3% perchloric acid. The acid extract was centrifuged, and duplicate samples of the clear supernatant were counted. Time zero uptake points were prepared by addition of stopper to the cells and ghosts prior to addition of medium containing sugar and radiolabel. Cells and ghosts were immediately processed. Radioactivity associated with cells and ghosts at time zero was subtracted from the activity associated with cells and ghosts following the uptake period. All uptakes were normalized to equilibrium uptake where cells and ghosts were exposed to sugar medium at 37 °C for 60 min prior to addition of stopper. Uptake assays were performed using solutions and tubes pre-equilibrated to 4 °C.

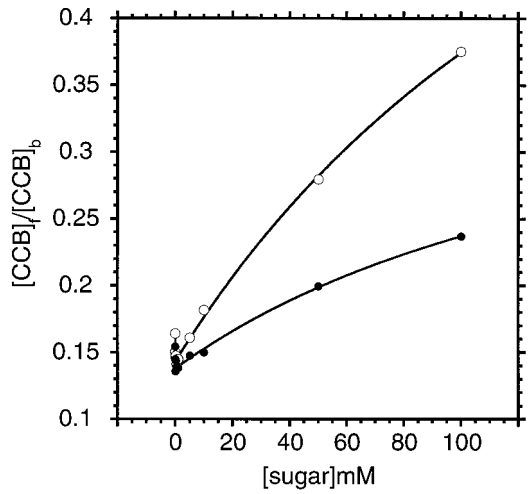

FIGURE 1: Effect of maltose (○) and maltotriose (●) on CCB binding to the glucose transporter in human erythrocytes at 24 °C. On the ordinate is shown the ratio of $[CCB]_{free}$ to $[CCB]_{bound}$. On the abscissa is shown the maltose or maltotriose concentration in millimolar. Each data point represents the average of at least four separate experiments made in triplicate. The curves drawn through the points were computed by nonlinear regression assuming CCB binding is described by eq 1 and that the mechanism of binding is described by Figure 6F in which $K_{d(app)}$ is given by eq 10. The following results were obtained. For maltose (○), B_{max} = 1052 nmol/L of cell water, K_L = 168 nM CCB, K_M = 29.3 μM, α = 0.87, β = 564, π =5.2, and R (coefficient of fit correlation) = 0.99. For maltotriose (●), B_{max} = 1003 nmol/L of cell water, K_L = 149 nM CCB, K_M = 32.3 μM, α = 0.89, β = 873, π = 2.7, and R (coefficient of fit correlation) = 0.99.

Curve Fitting Procedures. Equilibrium CCB binding and the concentration dependence of the sugar inhibition of the initial rates of 3OMG transport were analyzed by nonlinear regression using the software package KaleidaGraph 3.08d (Synergy Software, Reading, PA).

Analytical Procedures. Protein assays were carried out using the Pierce BCA protein assay procedure**.** Solutions for equilibrium CCB binding to and 3OMG transport by hypothetical carrier systems were obtained by making the rapid equilibrium assumption.

RESULTS

Cytochalasin B Binding. Cytochalasin B interacts with the substrate efflux site of the human red blood cell sugar transporter (*5*) to serve as a competitive inhibitor of exit (*13*) and as a noncompetitive inhibitor of sugar uptake (*14*). In the presence of 10 μM cytochalasin D [a competitive inhibitor of CCB binding to actin (*15*)], more than 98% of the saturable CCB binding to human red cells can be ascribed to CCB binding to GluT1 (*8*, *11*). Previous equilibrium CCB binding studies in this and other laboratories have examined the effects of extra- and intracellular sugars on CCB binding over the sugar concentration range of 1−250 mM (*7*, *11*, *16*, *17*). In the study presented here, we extend these analyses to lower sugar concentrations.

Figure 1 shows the concentration dependence of maltose and maltotriose modulation of equilibrium CCB binding to human erythrocytes. Maltose is not transported by human

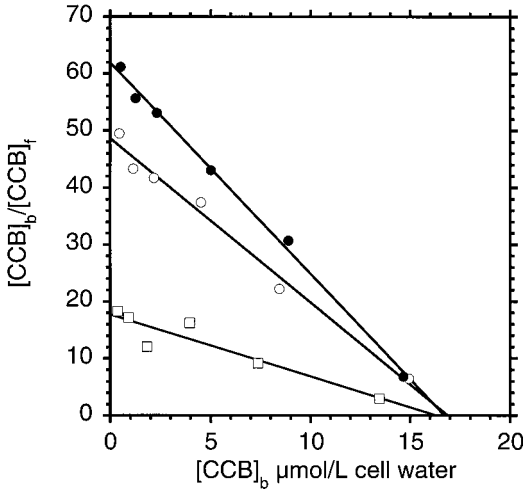

FIGURE 2: Scatchard analysis of the effect of 500 μM (●) and 10 mM (□) maltose on the concentration dependence of CCB binding to the glucose transporter in human erythrocytes at 24 °C. On the ordinate is shown the ratio of $[CCB]_{bound}$ to $[CCB]_{free}$. On the abscissa is shown $[CCB]_{bound}$ in micromoles per liter of cell water. Each data point represents the average of at least three separate experiments made in triplicate. The curves drawn through the points were computed by linear regression assuming CCB binding is described by eq 1. $K_{d(app)}$ is defined as 1/−slope, and B_{max} is defined as the *x*-intercept. The following results were obtained. For control (○), B_{max} = 1.69 μmol/L of cell water, $K_{d(app)}$ = 346.8 nM CCB, and *R* (coefficient of fit correlation) = 0.99. For 500 μM maltose (●), B_{max} = 1.67 μmol/L of cell water, $K_{d(app)}$ = 269.8 nM CCB, and *R* (coefficient of fit correlation) = 0.99. For 10 mM maltose (□), B_{max} = 1.63 μmol/L of cell water, $K_{d(app)}$ = 920.6 nM CCB, and *R* (coefficient of fit correlation) = 0.93.

Table 1: Effect of Maltose on CCB Binding to Red Cells

	$K_{d(app)}$[a] (nM)		
	control	500 μM maltose	100 mM maltose
	346.9	269.9	921
	431.3	332.4	1084
	368.8	236.3	1123
	384.0	317.9	1241
mean[b]	382.7	295.6[c]	1149.3[d]
standard error of the mean	18.8	29.9	47.2

[a] $K_{d(app)}$ for CCB binding to red blood cells was determined by Scatchard analysis of the concentration dependence of CCB binding (see Figure 2). Results are shown for four paired experiments where the level of CCB binding was measured in the absence and presence of 500 μM or 100 mM maltose. [b] Results are shown as the means. [c] Probability that $K_{d(app)}$ for binding in the presence of 500 μM maltose is identical to that for control binding < 0.0077 (two-tailed *t* test). [d] Probability that $K_{d(app)}$ for binding in the presence of 100 mM maltose is identical to that for control binding < 0.0014 (two-tailed *t* test).

erythrocytes (see below) and thus must modify CCB binding to GluT1 by acting at an exofacial site(s). Low concentrations (10−500 μM) of sugar increase the level of CCB binding, while higher concentrations inhibit CCB binding by an allosteric mechanism. Allosteric inhibition of CCB binding was expected on the basis of previous studies (*11*, *17*). Stimulation of binding was an unexpected result. Maltose is without significant effect on the maximum binding capacity of erythrocyte GluT1 for CCB but reduces $K_{d(app)}$ for CCB binding at low maltose concentrations and increases $K_{d(app)}$ for binding at high maltose concentrations (Figure 2 and Table 1).

Table 2: Effects of Sugars on CCB Binding to Red Cell GluT1

sugar[a]	B_{max}[b]	K_L[c]	K_M[d]	α[e]	β[f]	π[g]
24 °C						
maltose	1052	168	29.3	0.87	564	5.2
maltotriose	1003	149	32.2	0.89	873	2.7
maltotetraose	848	113	128	0.89	81	0.85
maltopentaose	965	153	18.8	0.88	902	1.1
4 °C						
maltose	846	135	71.8	0.86	88.6	2.17
D-glucose	799	144	31	0.82	4.1	1.02

[a] Effect of sugars on CCB binding to red blood cells was measured at 24 and 4 °C. This table summarizes the results of at least three experiments carried out with each sugar. The concentration dependence of sugar modulation of CCB binding was determined as described in the legends of Figures 1 and 3 and analyzed assuming the model of Figure 6F and using nonlinear regression analysis according to the expression $[CCB]_{free}/[CCB]_{bound} = [CCB]_{free}/B_{max} + K_{d(app)}/B_{max}$, where $K_{d(app)}$ is given by eq 10. The following parameters were obtained. [b] B_{max}, maximum CCB binding capacity of the human erythrocyte (nanomoles per liter of cell water). [c] K_L, K_d for CCB binding to GLuT1 in the absence of sugars (nanomolar). [d] K_M, K_d for sugar binding to the first sugar binding site in the absence of CCB (micromolar). [e] α, factor by which sugar binding at the first import site affects K_L for CCB binding to the export site. [f] β, factor by which sugar binding at the first import site affects K_M for sugar binding to import site 2. [g] π, factor by which sugar binding at import sites 1 and 2 affects K_L for CCB binding to the export site.

Several other nontransportable sugars known to interact with the GluT1 sugar import site (*5*, *7*, *18*) were also examined for their ability to modulate CCB binding over a wide range of sugar concentrations. Each sugar produced biphasic modulation of CCB binding (Table 2). Methyl α-D-glucopyranoside is without effect on CCB binding to erythrocytes over the concentration range of 0.1−100 mM. The effects of three transportable sugars were also examined (Figure 3). Unlike the nontransportable sugars, incubation of erythrocytes with a transported sugar leads to equilibration of cytosol with extracellular sugar. Biphasic modulation of CCB binding by a transported sugar could therefore reflect sugar interaction with GluT1 sugar import and sugar export sites (*11*, *18*).

We therefore compared the effects of D-glucose on CCB binding at 24 °C (where D-glucose rapidly equilibrates between the interstitium and the cytosol) and at 4 °C [where D-glucose is restricted to the extracellular space (*8*, *11*)]. This experiment was also performed using the nontransported but import site reactive sugar, maltose. At ice temperature, low concentrations of D-glucose (<0.5 mM) increase the level of CCB binding to red cells but higher concentrations restore CCB binding to control levels (Figure 3). Red cells equilibrated with D-glucose exhibit inhibition of CCB binding at both ice temperature and 24 °C. These data indicate that intracellular D-glucose inhibits CCB binding but that increasing concentrations of extracellular D-glucose stimulate and then restore binding to basal levels. Extracellular maltose modulation of CCB binding at ice temperature resembles that produced at 24 °C. In this instance, however, the concentration dependence of CCB binding modulation is shifted to lower sugar concentrations.

Close examination of the concentration dependence of maltose modulation of CCB binding indicates variations between units of blood. We considered the possibility that variations in erythrocyte metabolic status could account for this behavior. We therefore hypotonically lysed human

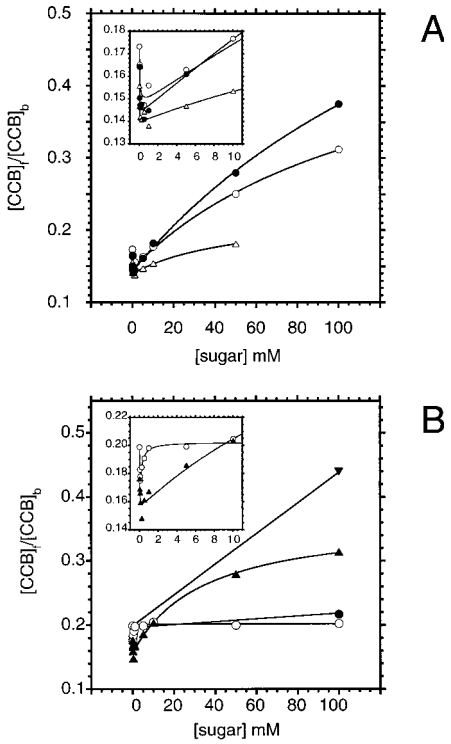

FIGURE 3: Effect of nontransportable and transportable sugars on CCB binding to the glucose transporter in human erythrocytes at 24 (A) or 4 °C (B). (A) On the ordinate is shown the ratio of $[CCB]_{free}$ to $[CCB]_{bound}$. On the abscissa is shown the sugar concentration in millimolar. Each data point represents the average of at least four separate experiments made in triplicate. Cells were equilibrated with sugars for 1 h prior to CCB binding determinations. The sugars that were used were maltose (●), D-glucose (○), and D-galactose (△). The curves drawn through the points were computed by nonlinear regression assuming CCB binding is described by eq 1 and that the mechanism of binding is described by Figure 6F in which $K_{d(app)}$ is given by eq 10. The following results were obtained. For maltose (●), B_{max} = 965 nmol/L of cell water, K_L = 153.4 nM CCB, K_M = 28.39 μM, α = 0.87, β = 580, π = 5.2, and R (coefficient of fit correlation) = 0.99. For D-glucose (○), B_{max} = 967 nmol/L of cell water, K_L = 163 nM CCB, K_M = 131 μM, α = 0.84, β = 131.9, π = 3.0, and R (coefficient of fit correlation) = 0.99. For D-galactose (△), B_{max} = 995 nmol/L of cell water, K_L = 150 nM CCB, K_M = 34.2 μM, α = 0.89, β = 454.1, π = 1.45, and R (coefficient of fit correlation) = 0.99. These analyses assume that the transported sugars do not penetrate the cells. The inset in panel A explodes the ordinate and abscissa to more clearly illustrate data in the sugar concentration range 0 to 10 mM. (B) On the ordinate is shown the ratio of $[CCB]_{free}$ to $[CCB]_{bound}$. On the abscissa is shown the sugar concentration in millimolar. Each data point represents the average of at least four separate experiments made in triplicate. Cells were equilibrated with sugar-free, ice-cold saline prior to mixing with ice-cold saline containing sugar and CCB for 2 min prior to binding determinations at 4 °C. The sugars that were used were maltose (▲) and D-glucose (○). The curves drawn through the points were computed by nonlinear regression assuming CCB binding is described by eq 1 and that the mechanism of binding is described by Figure 6F in which $K_{d(app)}$ is given by eq 10. The following results were obtained. For maltose (▲), B_{max} = 846 nmol/L of cell water, K_L = 134.7 nM CCB, K_M = 56.3 μM, α = 0.88, β = 122.1, π = 2.2, and R (coefficient of fit correlation) = 0.99. For D-glucose (○), B_{max} = 799 nmol/L of cell water, K_L = 144 nM CCB, K_M = 31 μM, α = 0.51, β = 4.1, π = 1.02, and R (coefficient of fit correlation) = 0.99. The black circles (●) and the inverted black triangles (▼) represent a paired experiment in triplicate in which the level of binding was measured in the presence of extracellular D-glucose alone (●) or intracellular D-glucose alone (▼). The inset of panel B explodes the ordinate and abscissa to more clearly illustrate data in the sugar concentration range from 0 to 10 mM.

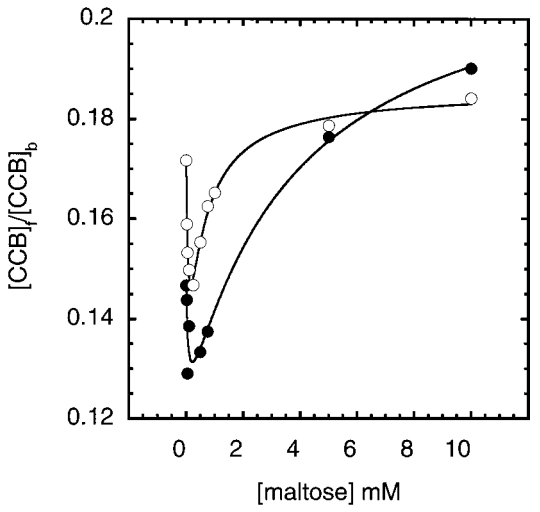

FIGURE 4: Effect of maltose on CCB binding to the glucose transporter in resealed human erythrocytes ghosts at 24 °C lacking (○) or containing (●) 4 mM MgATP. On the ordinate is shown the ratio of $[CCB]_{free}$ to $[CCB]_{bound}$. On the abscissa is shown the maltose concentration in millimolar. Each data point represents the average of at least four separate experiments made in triplicate. The curves drawn through the points were computed by nonlinear regression assuming CCB binding is described by eq 1 and that the mechanism of binding is described by Figure 6F in which $K_{d(app)}$ is given by eq 10. The following results were obtained. For 0 mM ATP (○), B_{max} = 1121 nmol/L of cell water, K_L = 187 nM CCB, K_M = 224.6 μM, α = 0.70, β = 0.7, π = 1.1, and R (coefficient of fit correlation) = 0.99. For 4 mM MgATP (●), B_{max} = 1228 nmol/L of cell water, K_L = 175 nM CCB, K_M = 168 μM, α = 0.82, β = 6.2, π = 1.5, and R (coefficient of fit correlation) = 0.98.

erythrocytes and resealed the resulting membranes in the presence or absence of MgATP and assessed the effects of intracellular ATP on the extracellular maltose modulation of CCB binding. These experiments demonstrate that ATP depletion reduces the concentration of extracellular maltose necessary for reversal of maltose stimulation of CCB binding (Figure 4).

Sugar Transport. Extracellular maltose and maltotriose (1−100 mM) inhibit 3OMG uptake by human red blood cells. We were surprised to observe, however, that lower concentrations of maltose or maltotriose stimulate 3OMG uptake (Figure 5). This behavior was also observed for several nontransported and transported sugars (Table 3). Low concentrations of maltose serve to reduce $K_{m(app)}$ for 3OMG uptake [control, V_{max} = 86 ± 8 μmol L of cell water^{-1} min^{-1}, $K_{m(app)}$ = 607 ± 179 μM; with 250 μM maltose, V_{max} = 75 ± 5 μmol L of cell water^{-1} min^{-1}, $K_{m(app)}$ = 161 ± 23 μM]. Higher (inhibitory) concentrations increase $K_{m(app)}$ for net 3OMG influx [with 10 mM maltose, V_{max} = 125 ± 24 μmol L of cell water^{-1} min^{-1}, $K_{m(app)}$ = 1158 ± 381 μM].

Maltose is not transported by human red blood cells. Incubation of erythrocytes with [^{3}H]maltose at 37 °C for 2 h hours leads to less than 1% equilibration of the 3OMG space of the red cell (Table 4). Addition of 100 μM or 100 mM 3OMG is without effect on maltose uptake.

DISCUSSION

The study presented here describes two novel actions of low concentrations of extracellular sugar on human erythrocyte sugar transporter function. GluT1-mediated CCB

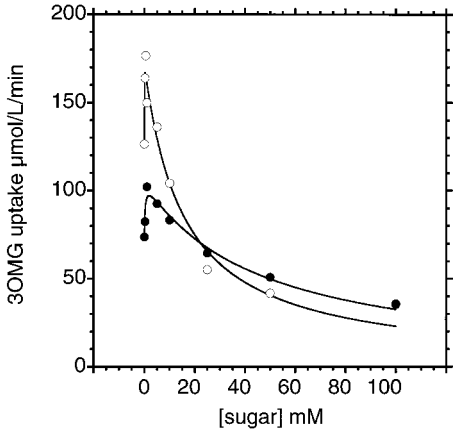

FIGURE 5: Effect of maltose (○) and maltotriose (●) on 100 μM 3OMG uptake by human erythrocytes at 4 °C. On the ordinate is shown the rate of 3OMG uptake in micromoles of 3OMG per liter of cell water per minute. On the abscissa is shown the maltose or maltotriose concentration in millimolar. Each data point represents the average of at least four separate experiments made in triplicate. The curves drawn through the points were computed by nonlinear regression assuming 3OMG transport is described by eq 3 and that the mechanism of binding is described by Figure 6G in which V_{max} is given by eq 11 and $K_{m(app)}$ is given by eq 12. The following results were obtained. For maltose (○), $V_1 = 165$ μmol L of cell water^{-1} min^{-1}, $V_2 = 663$ μmol L of cell water^{-1} min^{-1}, $V_3 = 299$ μmol L of cell water^{-1} min^{-1}, $K_S = 314$ μM 3OMG, $K_M = 32$ μM maltose, $\delta = 0.53$, $\beta = 102$, $\gamma = 0.23$, and R (coefficient of fit correlation) = 0.99. For maltotriose (●), $V_1 = 95$ μmol L of cell water^{-1} min^{-1}, $V_2 = 460$ μmol L of cell water^{-1} min^{-1}, $V_3 = 299$ μmol L of cell water^{-1} min^{-1}, $K_S = 376$ μM 3OMG, $K_M = 586$ μM, $\delta = 0.45$, $\beta = 25$, $\gamma = 0.49$, and R (coefficient of fit correlation) = 0.99.

Table 3: Effects[a] of Sugars on 3OMG Transport by Red Cells

sugar[b]	V_1[c]	V_2[d]	V_3[e]	K_S[f]	δ[g]	K_M[h]	γ[i]	β[j]
maltose	165	663	299	314	0.53	32	0.23	102.2
maltotriose	95	460	300	376	0.45	586	0.49	24.8
ethylideneglucose	93	327	181	462	0.4	57	0.16	14.7
galactose	87	286	149	460	0.53	59	0.31	7.3
D-glucose	96	491	119	405	0.35	64	0.36	5.6
mean[k]	107	445		403	0.45			
standard error of the mean	15	17		28	0.04			

[a] The rate of 3OMG (100 μM) uptake by erythrocytes at 4 °C was measured in the presence and absence of various sugars (e.g., see Figure 5). [b] Data for each test sugar represent the averaged results of at least three separate experiments. Data were analyzed by nonlinear regression assuming the transport mechanism of Figure 6G and using eqs 3, 11, and 12. The following parameters were obtained. [c] V_1, maximum rate of 3OMG transport through a transporter occupied by only a single extracellular 3OMG molecule. [d] V_2, maximum rate of 3OMG transport through a transporter occupied by two extracellular 3OMG molecules. [e] V_3, maximum rate of 3OMG transport through a transporter occupied by one extracellular 3OMG molecule and one extracellular test sugar molecule. [f] K_S, dissociation constant for 3OMG binding to an unoccupied transporter. [g] δ, factor by which binding of the first 3OMG molecule affects the dissociation constant for binding a second 3OMG molecule. [h] K_M, dissociation constant for the test sugar molecule binding to an unoccupied transporter. [i] γ, factor by which binding of a test sugar molecule affects K_S. [j] β, factor by which binding of the first test sugar molecule affects K_M. [k] Means were calculated for V_1, V_2, K_S, and δ.

binding and 3OMG uptake are stimulated when low concentrations of certain extracellular sugars are present but are unaffected or inhibited in the presence of higher concentrations of these sugars.

Sugar transport by human erythrocytes is consistent with a mechanism in which the glucose transporter presents sugar

Table 4: Transport of Sugars by Human Red Cells

sugar	rate of uptake[a] (μmol L^{-1} min^{-1}) control	with 500 μM D-glucose
3OMG	78	25
maltose	2	2

[a] The rate of sugar (3OMG or maltose) uptake (100 μM at 4 °C) was measured in quadruplicate in the absence (control) or presence of 500 μM D-glucose.

import and sugar export pathways simultaneously (*3*, *5*, *14*). Some clues to the physical basis of this behavior were obtained from the demonstration that the sugar transporter is comprised of four copies of the sugar transport protein GluT1 (*6*, *19*). Each GluT1 molecule functions as a basic catalytic unit (*6*, *20*, *21*) and alternates between two functional states. The e2 state is import competent and presents a substrate binding site to extracellular sugar. The e1 state is export competent and presents a substrate binding site to intracellular sugar. Subunit conformational changes between the e1 and e2 states represent those steps mediating translocation of bound sugar between the cytosol and the interstitium and vice versa (*22*, *23*).

The structural topology of each GluT1 protein (subunit) within the transport complex is identical and invariant [amino and carboxyl termini are cytosolic (*24*)]. It has been hypothesized, however, that cooperative interactions between subunits produce an antiparallel, functional arrangement of subunits (*6*). Thus, when one subunit presents a sugar import (e2) site, the adjacent subunit must present a sugar export (e1) site and vice versa. In this way, each transporter would present two sugar import and two sugar export sites at any time. This study presents the first evidence that each glucose transporter presents at least two sugar import sites and at least one sugar export site at any instant.

The inhibitory effects of high concentrations of extracellular sugars on CCB binding and sugar uptake reported here were expected on the basis of previous studies (*7*, *11*, *13*, *14*, *17*). Transported (e.g., D-glucose and D-galactose) and nontransported but GluT1 reactive sugars (e.g., maltose and maltotriose) serve as competitive inhibitors of net 3OMG uptake when present in the extracellular medium because these sugars compete for binding at a common (import) site (*14*). Extracellular sugars modulate CCB binding at the sugar export site by promoting cooperativity between the e1 and e2 subunits. For example, extracellular maltose occupation of the e2 site on one GluT1 subunit reduces the affinity of the e1 site on an adjacent GluT1 subunit for CCB and vice versa (*5*, *6*, *11*, *17*). Extracellular D-glucose is known to be without effect on the CCB binding affinity (*8*, *11*).

The actions of low sugar concentrations on transport and CCB binding were unexpected. Previous studies have not systematically examined this concentration range for the sugars used in the study presented here (*7*, *11*, *14*). Maltose and its oligomers produce increased levels of CCB binding at low concentrations (10−500 μM) and thereafter reduce the level of CCB binding. Both behaviors are very revealing with respect to import site−import site interactions and import site−export site interactions.

Inhibition of CCB binding at high concentrations of sugar is inconsistent with simple competitive inhibition. If CCB and maltose were to compete for binding at identical sites

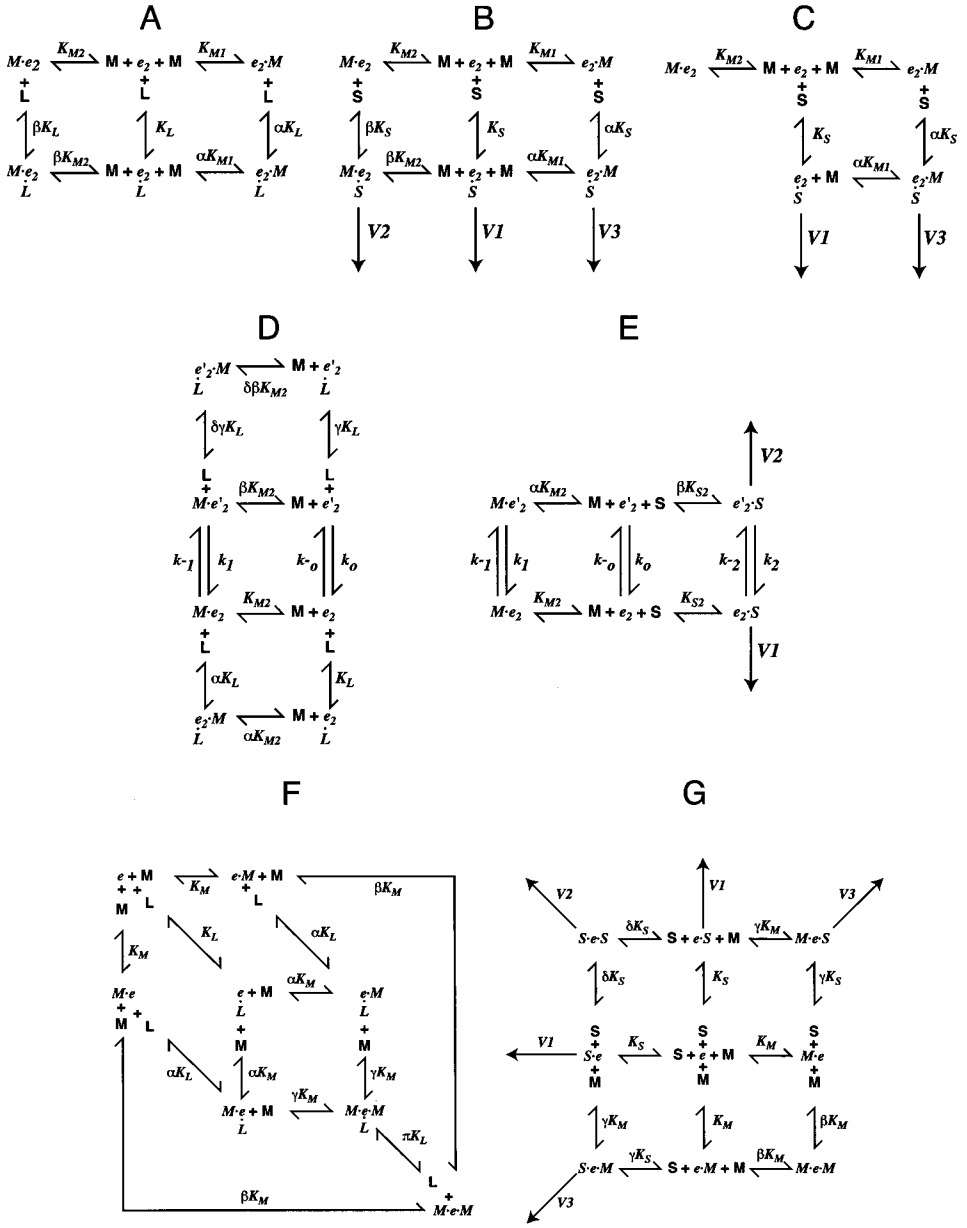

FIGURE 6: Models for maltose modulation of CCB binding to and 3OMG transport by the sugar transporter. Each panel is a King−Altman representation. Three types of models are represented: noncatalytic maltose binding site models (A−C), an activation−relaxation model (D and E), and a carrier with two uptake sites (F and G). With the noncatalytic maltose binding site models, the carrier (e2) presents mutually exclusive high- and low-affinity maltose binding sites. Thus, the carrier can exist as M−e2 or as e2−M. Dissociation constants for maltose (M) interaction with e2 are K_{M_1} and K_{M_2}. CCB (L) can interact with e2 with the dissociation constant K_L. Binding to M−e2 or e2−M is described by dissociation constant βK_L or αK_L, respectively. Transported sugar (S) interacts with e2, M−e2, or e2−M (panel B) with dissociation constant K_S, βK_S, or αK_S to form e2(S), M−e2(S), or (S)e2−M, respectively, and is subsequently translocated into the cell at rate V_1, V_2, or V_3, respectively. In panel C, one maltose binding site corresponds to the sugar uptake site and is thus mutually exclusive with e2(S). With the activation−relaxation model of Naftalin (*10*), the carrier exists in a basal (e2) or activated (e′2) state and isomerizes between these states at rates described by the first-order rate constants k_o and k_{-o} (panels D and E). Maltose binding to e2 (described by dissociation constant K_{M_2}) accelerates the rate of carrier activation ($k_{-1} > k_{-o}$). Transported sugar (S) binds to e2 and e′2 with dissociation constants K_{S_2} and βK_{S_2}, respectively, and is transported more rapidly by the activated complex than by the basal complex ($V_2 > V_1$). With the carrier containing two sugar uptake sites (panels F and G), maltose and transported sugar (S) compete for binding at either of the two sugar uptake sites, although only S is translocated and maltose occupation of one uptake site does not prevent S translocation through the second site. CCB (L) can bind to e, M−e, e−M, or M−e−M with dissociation constants K_L, αK_L, αK_L, and πK_L, respectively. Maltose occupation of one uptake site affects the dissociation constants for maltose or S occupation of the remaining site by factor β or γ, respectively. Rates of S translocation through e−S (or S−e), S−e−S, and S−e−M (or M−e−S) are given by V_1, V_2, and V_3, respectively.

or at different but mutually exclusive sites, maltose inhibition of CCB binding would be of the linear competitive type (*7*, *25*) in which the ratio of free CCB concentration to bound CCB concentration increases linearly with maltose concentration. The relationship is, in fact, nonlinear (see Figure 1 here; *11*, *17*) and, rather, is consistent with negative cooperativity between ligand binding sites. Thus, if an external (e2) site is occupied by maltose, the internal CCB binding site (e1) exhibits a reduced affinity for CCB and vice versa.

How is an increased level of CCB binding explained? If the unoccupied glucose transporter has a high affinity for

extracellular sugar, saturation of import sites would require relatively low maltose concentrations. If occupation of this high-affinity e2 site by maltose were to promote increased affinity for CCB at an e1 site, the level of CCB binding at limiting CCB concentrations would be increased by low maltose concentrations. How then do we account for the biphasic action of maltose on CCB binding? Could two maltose-binding sites exist in which occupancy of one site promotes CCB binding while occupancy of a second inhibits CCB binding? We modeled this possibility in several ways.

Our first approach was to assume that the glucose transporter presents two mutually exclusive sugar import (e2) sites (Figure 6A). Addition of maltose to the high-affinity e2 site increases the level of CCB binding at the export site and prevents maltose binding at the low-affinity e2 site. Addition of maltose to the low-affinity e2 site inhibits CCB binding at the export site and ablates maltose binding at the high-affinity e2 site. Equilibrium CCB binding follows simple Michaelis−Menten kinetics in which

$$[\mathrm{CCB}]_{\mathrm{bound}} = \frac{[\mathrm{CCB}]B_{\mathrm{max(app)}}}{K_{\mathrm{d(app)}} + [\mathrm{CCB}]} \tag{1}$$

where $B_{\mathrm{max(app)}}$ = the GluT1 concentration, and

$$K_{\mathrm{d(app)}} = K_{\mathrm{L}}\left(\frac{1 + \frac{M}{K_{\mathrm{M_1}}} + \frac{M}{K_{\mathrm{M_2}}}}{1 + \frac{M}{\alpha K_{\mathrm{M_1}}} + \frac{M}{\beta K_{\mathrm{M_2}}}}\right) \tag{2}$$

where α and β are cooperativity constants indicating positive or negative cooperative effects of CCB binding on maltose binding at sites 1 and 2 (see Figure 6A) and M is the extracellular maltose concentration. Thus $K_{\mathrm{d(app)}}$ alone is affected by the presence of maltose. This model predicts that the high-affinity term dominates and that biphasic behavior is not observed.

This model also cannot account for the effects on sugar uptake (Figure 6B) because maltose would compete directly for 3OMG binding at each import site. 3OMG transport is described by the equation

$$[\mathrm{3OMG}]_{\mathrm{uptake}} = \frac{V_{\mathrm{max(app)}}[\mathrm{3OMG}]_{\mathrm{o}}}{K_{\mathrm{m(app)}} + [\mathrm{3OMG}]_{\mathrm{o}}} \tag{3}$$

where $[\mathrm{3OMG}]_{\mathrm{o}}$ is the extracellular 3OMG concentration. The maximum rate of transport $[V_{\mathrm{max(app)}}]$

$$= [\mathrm{GluT1}]\frac{V_1 + M\left(\frac{V_2}{\beta K_{\mathrm{M_2}}} + \frac{V_3}{\alpha K_{\mathrm{M_1}}}\right)}{1 + \frac{M}{\beta K_{\mathrm{M_2}}} + \frac{M}{\alpha K_{\mathrm{M_1}}}} \tag{4}$$

and the Michaelis constant for transport

$$K_{\mathrm{m(app)}} = K_{\mathrm{S}}\frac{1 + \frac{M}{K_{\mathrm{M_2}}} + \frac{M}{K_{\mathrm{M_1}}}}{1 + \frac{M}{\beta K_{\mathrm{M_2}}} + \frac{M}{\alpha K_{\mathrm{M_1}}}} \tag{5}$$

where V_2 is V_{max} for 3OMG transport through the M−e2(S) complex and V_3 is V_{max} for 3OMG transport through the (S)e2−M complex. Because the ternary M−e2−M complex cannot be formed, the high-affinity state will dominate and transport will be either stimulated (e.g., $V_2 > V_1$) or inhibited (e.g., $V_2 < V_1$) but not both.

The model can be modified, however, to allow for the possibility that both mutually exclusive maltose binding sites are noncatalytic, allosteric sites and allow the formation of a carrier−maltose−3OMG ternary complex (Figure 6B). If 3OMG transport through the ternary complex is faster or slower than transport through the carrier−3OMG complex, the addition of maltose can affect 3OMG transport. However, as with CCB binding, transport can be stimulated or inhibited by maltose but biphasic behavior is not permitted.

A variant of this scheme allows for 3OMG and maltose competition for a single import site but also for maltose binding at an additional allosteric site (Figure 6C). 3OMG transport is described by eq 3.

The maximum rate of transport

$$V_{\mathrm{max(app)}} = [\mathrm{GluT1}]\frac{V_1 + \frac{V_3 M}{\alpha K_{\mathrm{M_1}}}}{1 + \frac{M}{\alpha K_{\mathrm{M_1}}}} \tag{6}$$

and the Michaelis constant for transport

$$K_{\mathrm{m(app)}} = K_{\mathrm{S}}\frac{1 + \frac{M}{K_{\mathrm{M_2}}} + \frac{M}{K_{\mathrm{M_1}}}}{1 + \frac{M}{\alpha K_{\mathrm{M_1}}}} \tag{7}$$

Again, transport can be stimulated or inhibited by maltose, but biphasic behavior is not permitted because a ternary GluT1−M−M complex is not permitted.

A rather different mechanism was also considered. Naftalin (*10*) has made the interesting suggestion that sugar binding to the sugar import site causes the transporter to become activated. Thus, maltose might associate with an import site and activate the carrier and, following maltose dissociation, will leave the carrier in a transiently activated state (e′2, Figure 6D). Thus, any available transportable sugar might be transported more readily in the presence of low concentrations of maltose than in its absence (Figure 6E). As maltose levels rise, however, they will competitively inhibit carrier interaction with transportable sugar and thus lead to transport inhibition. Similarly, CCB binding to the export site of the "activated" carrier might be characterized by a higher affinity than binding to the ground state carrier (Figure 6D).

Cytochalasin B binding to this carrier (Figure 6D) is described by eq 1 where $B_{max(app)} = [GluT1]$, and

$$K_{d(app)} = K_L\left[\frac{\left(1+\frac{M}{K_M}\right)\left(k_o+\frac{k_1M}{\beta K_M}\right)+\left(1+\frac{M}{\beta K_M}\right)\left(k_{-o}+\frac{k_{-1}M}{K_M}\right)}{\left(1+\frac{M}{\alpha K_M}\right)\left(k_o+\frac{k_1M}{\beta K_M}\right)+\left(1+\frac{M}{\delta\beta K_M}\right)\left(\frac{k_{-o}}{\gamma}+\frac{k_{-1}M}{\gamma K_M}\right)}\right] \quad (8)$$

The rate of 3OMG uptake, v, by this mechanism (Figure 6E) is described by

$$v = \frac{S(Q+S)}{Q_{00}+SQ_{21}+SSQ_e} \quad (9)$$

where

$$Q = \frac{\left[\frac{V_1k_{-o}}{\beta}+V_2k_o+M\left(\frac{V_2k_1}{\alpha K_M}+\frac{V_2k_{-1}}{\beta K_M}\right)\right]\beta K_S}{V_1k_{-2}+V_2k_2}$$

$$Q_{00} = \frac{\left\{k_o+k_{-o}+M\left[\frac{1}{K_M}\left(k_o+\frac{k_{-o}}{\alpha}+\frac{k_1}{\alpha}+k_{-1}\right)+\frac{M}{\alpha K_M{}^2}(k_1+k_{-1})\right]\right\}\beta K_S{}^2}{V_1k_{-2}+V_2k_2}$$

$$Q_{21} = \frac{\left\{k_o+\frac{k_{-o}}{\beta}+\frac{k_2}{\beta}+k_{-2}+\frac{M}{K_M}\left[\frac{k_1}{\alpha}+\frac{k_{-1}}{\beta}+\frac{k_2}{\beta}+\frac{k_{-2}}{\alpha}\right]\right\}\beta K_S}{V_1k_{-2}+V_2k_2}$$

$$Q_e = \frac{k_{-1}+k_2}{V_1k_{-2}+V_2k_2}$$

with the constraints (*26*)

$$\alpha = \frac{k_{-0}k_1}{k_0k_{-1}} \text{ and } \beta = \frac{k_{-0}k_2}{k_0k_{-2}}$$

As with the previous models, high-affinity maltose binding terms dominate, and since a ternary carrier−maltose−3OMG complex is not permitted, this model is unable to predict biphasic CCB binding and biphasic sugar transport with increasing maltose concentrations.

Our third approach was to assume that the glucose transporter presents two coexistent sugar import (e2) sites (Figure 6F). In the absence of extracellular ligand, both e2 sites have a high affinity for maltose. Addition of maltose to either of the high-affinity e2 sites reduces $K_{d(app)}$ for CCB binding at the export site by the factor α and reduces the affinity of the second e2 site for maltose by the factor β. Addition of the second maltose molecule at the low-affinity e2 site increases $K_{d(app)}$ for CCB binding at the export site by the factor π.

Equilibrium CCB binding to this carrier is described by eq 1 where $B_{max(app)} = [GluT1]$ and

$$K_{d(app)} = K_L\left(\frac{1+\frac{2M}{K_M}+\frac{M^2}{\alpha K_MK_M}}{1+\frac{2M}{\beta K_M}+\frac{M^2}{\alpha\pi K_MK_M}}\right) \quad (10)$$

This model permits biphasic modulation of CCB binding because the carrier can be occupied by either one or two maltose molecules and the CCB binding properties of each form are different. This model can also account for the effects of maltose on 3OMG uptake (Figure 6G) if 3OMG translocation through a carrier occupied by a single maltose molecule and a single 3OMG molecule is faster than 3OMG translocation through a carrier occupied only by a single 3OMG molecule. Addition of the second maltose molecule inhibits 3OMG uptake because there are only two possible uptake sites and maltose occupies both.

3OMG transport is described by eq 3 in which

$$V_{max(app)} = [GluT1]\frac{2V_1+\frac{V_2S}{\delta K_S}+\frac{2V_3M}{\gamma K_M}}{2+\frac{S}{\delta K_S}+\frac{2M}{\gamma K_M}} \quad (11)$$

and

$$K_{m(app)} = K_S\frac{1+\frac{2M}{K_M}+\frac{M^2}{\beta K_MK_M}}{2+\frac{S}{\delta K_S}+\frac{2M}{\gamma K_M}} \quad (12)$$

Since maltose (100 μM) is not transported by red cells in the presence or absence of low concentrations of 3OMG, we must conclude that 3OMG transport through one import site of the carrier is independent of the translocational competency of the second e2 site.

Analysis of our findings within the context of this model indicates that the first sugar molecule binds to unoccupied transporter with significantly greater affinity (30−2000-fold depending on the sugar; $\beta \geq 30-2000$) than does the second sugar. Maltose binding data are consistent with our previous findings (*6*, *11*, *17*) that occupancy of both extracellular maltose binding sites increases $K_{d(app)}$ for CCB binding at the export site by 5-fold ($\pi = 5$). We now know, however, that occupancy of only one of the two extracellular maltose binding sites reduces $K_{d(app)}$ for CCB binding at the export site by 15% ($\alpha \approx 0.85$). A similar result is obtained for occupancy of the first sugar binding site by D-glucose (a transported sugar; $\alpha \approx 0.85$). However, unlike that of its nontransportable counterparts, D-glucose occupancy of both extracellular sites is without effect on CCB binding ($\pi = 1$). A similar result has been reported previously for the effects of saturating extracellular D-glucose concentrations on CCB binding (*8*, *11*). Occupancy of a single import site by the nontransportable sugar maltose increases V_{max} for 3OMG transport through the remaining import site by 1.75-fold ($V_3/V_1 = 1.75$). Occupancy of the first import site by other sugars (nontransportable and transportable) increases

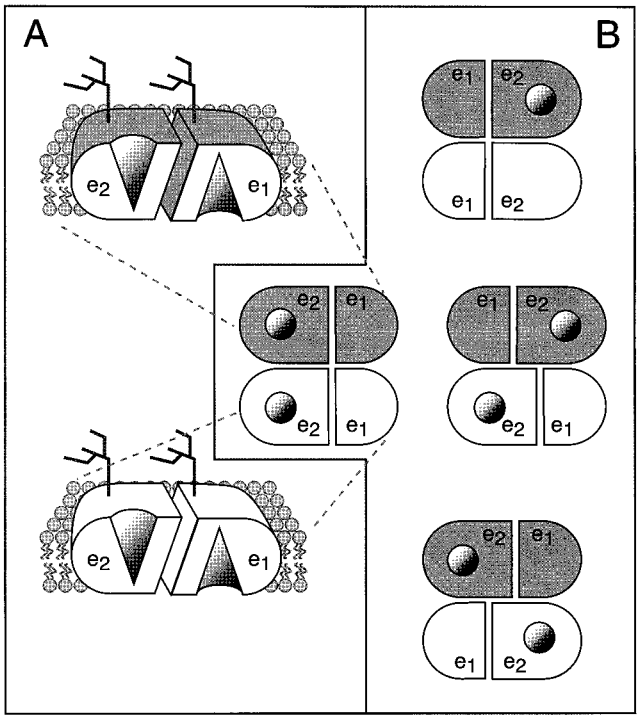

FIGURE 7: Model for GluT1-mediated sugar transport in human red blood cells. The glucose transporter is a complex of four GluT1 proteins and functions as a dimer of GluT1 dimers. In each dimer, if one subunit presents a sugar uptake (e2) site, its partner must present a sugar export (e1) site. Thus, each dimer can exist as e2−e1 or as e1−e2. This figure represents the transporter as two dimers as viewed from the extracellular milieu looking down on the cell membrane (section B). One dimer of the tetramer is gray and the other white. The cut-outs to the left of the (e2−e1)−(e2−e1) tetramer (section A) illustrate this model as viewed through the plane of the membrane bilayer. Although the occupancy state of each dimer may be communicated across the dimer−dimer interface to affect the occupancy of the cognate dimer, each dimer can translocate substrate independently of its partner. Thus, four possible carrier configurations are permitted: (e2−e1)−(e2−e1), (e1−e2)−(e2−e1), (e2−e1)−(e1−e2), and (e1−e2)−(e1−e2).

V_{max} for 3OMG transport via the second import site by 2−3-fold. D-Glucose is without effect on 3OMG transport. Thus, even when one e2 subunit is inhibited through occupancy by a nontransportable substrate, the second e2 subunit can undergo the e2 → e1 conformational change required for transport.

These findings indicate that although transporter subunits interact with positive or negative cooperativity, import (e2) subunits can be catalytically uncoupled from adjacent e2 subunits but not from export (e1) subunits. Thus, tetrameric GluT1 might be more accurately described as a dimer of two GluT1 dimers (Figure 7) in which each dimer is comprised of functionally antiparallel GluT1 subunits (e2−e1 or e1−e2). When one subunit in any given dimer presents an e1 conformation, its partner must present an e2 conformation and vice versa. This reduces the CCB binding capacity of each dimer to 1 mol of CCB bound per 2 mol of GluT1 (*6*). This also permits accelerated exchange transport in which unidirectional sugar fluxes (uptake or efflux) proceed more rapidly when sugar is present at both sides of the membrane (e1 and e2 subunits are occupied by sugar). Communication across the dimer−dimer interface permits the occupancy state of subunits in one dimer to alter the affinity of subunits within the second dimer for ligands. Thus, maltose occupancy of a single e2 subunit reduces $K_{d(app)}$ for CCB binding to e1 subunits and increases $K_{d(app)}$ for 3OMG binding to and the rate of 3OMG translocation through the remaining e2 subunit. In this way, the unoccupied e2 subunit of the second dimer can catalyze sugar import when the e2 subunit of the first dimer is inhibited by maltose. Maltose occupancy of both e2 subunits of the tetramer increases $K_{d(app)}$ for CCB binding at e1 sites and arrests transport completely.

CONCLUSION

This study demonstrates that low concentrations of extracellular substrate or inhibitor increase the levels of GluT1-mediated sugar transport and CCB binding while higher concentrations inhibit transport and ligand binding. These data can only be explained if the glucose transporter presents two exofacial sugar binding sites that interact cooperatively with each other and with the sugar export (CCB binding) site. Because occupancy of both extracellular sites competitively inhibits sugar import, at least one of these sites must be a sugar import site. The simplest model suggests that both sites are sugar import sites. These findings also suggest that one sugar import site can mediate sugar uptake under conditions where the other uptake site is locked in an inhibited state (liganded with maltose).

REFERENCES

1. Mueckler, M., Caruso, C., Baldwin, S. A., Panico, M., Blench, I., Morris, H. R., Allard, W. J., Lienhard, G. E., and Lodish, H. F. (1985) *Science 229*, 941−945.
2. Zottola, R. J., Cloherty, E. K., Coderre, P. E., Hansen, A., Hebert, D. N., and Carruthers, A. (1995) *Biochemistry 34*, 9734−9747.
3. Baker, G. F., and Naftalin, R. J. (1979) *Biochim. Biophys. Acta 550*, 474−484.
4. Baker, G. F., and Widdas, W. F. (1973) *J. Physiol. (London) 231*, 143−165.
5. Sultzman, L. A., and Carruthers, A. (1999) *Biochemistry 38*, 6640−6650.
6. Hebert, D. N., and Carruthers, A. (1992) *J. Biol. Chem. 267*, 23829−23838.
7. Gorga, F. R., and Lienhard, G. E. (1981) *Biochemistry 20*, 5108−5113.
8. Cloherty, E. K., Heard, K. S., and Carruthers, A. (1996) *Biochemistry 35*, 10411−10421.
9. Baker, G. F., and Widdas, W. F. (1988) *J. Physiol. (London) 395*, 57−76.
10. Naftalin, R. J. (1998) *Exp. Physiol. 83*, 253−258.
11. Helgerson, A. L., and Carruthers, A. (1987) *J. Biol. Chem. 262*, 5464−5475.
12. Levine, K. B., Cloherty, E. K., Fidyk, N., and Carruthers, A. (1998) *Biochemistry 37*, 12221−12232.
13. Basketter, D. A., and Widdas, W. F. (1978) *J. Physiol. (London) 278*, 389−401.
14. Carruthers, A., and Helgerson, A. L. (1991) *Biochemistry 30*, 3907−3915.
15. Jung, C. Y., and Rampal, A. L. (1977) *J. Biol. Chem. 252*, 5456−5463.
16. Sogin, D. C., and Hinkle, P. C. (1980) *Biochemistry 19*, 5417−5420.
17. Coderre, P. E., Cloherty, E. K., Zottola, R. J., and Carruthers, A. (1995) *Biochemistry 34*, 9762−9773.
18. Gorga, F. R., and Lienhard, G. E. (1982) *Biochemistry 21*, 1905−1908.
19. Zottola, R. J., Cloherty, E. K., Coderre, P. E., Hansen, A., Hebert, D. N., and Carruthers, A. (1995) *Biochemistry 34*, 9734−9747.
20. Sogin, D. C., and Hinkle, P. C. (1978) *J. Supramol. Struct. 8*, 447−453.

21. Baldwin, S. A., Baldwin, J. M., and Lienhard, G. E. (1982) *Biochemistry 21*, 3836−3842.
22. Widdas, W. F. (1952) *J. Physiol. (London) 118*, 23−39.
23. Lieb, W. R., and Stein, W. D. (1974) *Biochim. Biophys. Acta 373*, 178−196.
24. Mueckler, M. (1994) *Eur. J. Biochem. 219*, 713−725.
25. Krupka, R. M., and Devés, R. (1981) *J. Biol. Chem. 256*, 5410−5416.
26. Segel, I. H. (1975) in *Enzyme Kinetics*, pp 161−162, Wiley, New York.

BI9918792